Published in final edited form as:
*Pflugers Arch*. 2014 August ; 466(8): 1571–1579. doi:10.1007/s00424-013-1385-y.

# A mutation in the extracellular domain of the α7 nAChR reduces calcium permeability

**José O. Colón-Sáez** and **Jerrel L. Yakel**
Laboratory of Neurobiology, National Institute of Environmental Health Science, National Institutes of Health, Department of Health and Human Services, PO Box 12233, Research Triangle Park, NC 27709, USA

Jerrel L. Yakel: yakel@niehs.nih.gov

## Abstract

The α7 neuronal nicotinic acetylcholine receptor (nAChR) displays the highest calcium permeability among the different subtypes of nAChRs expressed in the mammalian brain and can impact cellular events including neurotransmitter release, second messenger cascades, cell survival, and apoptosis. The selectivity for cations in nAChRs is thought to be achieved in part by anionic residues which are located on either side of the channel mouth and increase relative cationic concentration. Mutagenesis studies have improved our understanding of the role of the second transmembrane domain and the intracellular loop of the channel in ion selectivity. However, little is known about the influence that the extracellular domain (ECD) plays in ion permeation. In the α7 nAChR, it has been found that the ECD contains a ring of ten aspartates (two per subunit) that is believed to face the lumen of the pore and could attract cations for permeation. Using mutagenesis and a combination of electrophysiology and imaging techniques, we tested the possible involvement of these aspartate residues in the calcium permeability of the rat α7 nAChR. We found that one of these residues (the aspartate at position 44) appears to be essential since mutating it to alanine resulted in a decrease in amplitude for both whole cell and single-channel responses and in the complete disappearance of detectable calcium changes in most cells, which indicates that the ECD of the α7 nAChR plays a key role in calcium permeation.

### Keywords

Alpha 7 nAChR; Calcium permeability; Extracellular domain; Mutagenesis

## Introduction

Neuronal nicotinic acetylcholine receptors (nAChRs) are ligand-gated ion channels that play a major role in synaptic transmission in the nervous system. These receptors are pentameric complexes formed by combinations of α2–10 and β2–4 subunits, of which only the α7 and α9 subunits can form functional homopentamers. Each subunit contains a large N-terminal extracellular domain (ECD), which contains the ligand-binding site, followed by four


Correspondence to: Jerrel L. Yakel, yakel@niehs.nih.gov.

transmembrane domains (M1–4), a large intracellular loop, and a short extracellular C terminus. The interactions between the five M2 domains from the various subunits contribute to the formation of the cation-selective channel pore [1].

The two most common subtypes of nAChRs expressed in the brain, and particularly in the hippocampus, are composed of the α7 and α4β2 subtypes [22]. The subunit composition dictates channel function, and α7 receptors display a lower agonist affinity for the endogenous ligand acetylcholine (ACh), higher calcium permeability, and faster desensitization kinetics than α4β2 nAChRs. The α7 nAChRs display the highest calcium permeability among the nAChR expressed in the brain [5, 11], allowing them to play an important role in cellular events such as neurotransmitter release survival [37], and apoptosis [3]. They have also been implicated in neurodegenerative diseases such as Alzheimer's and Parkinson's diseases, and schizophrenia [30].

The selectivity for cations in nAChRs is thought to be achieved in part by anionic residues located on either side of the channel mouth, which stabilizes and increases the relative ionic concentration [44]. Mutagenesis studies looking at the M2 domain and the intracellular loop of the channel have uncovered key residues involved in channel selectivity and permeation [7]. For example, when three residues in the M2 domain of the α7 nAChR were mutated, they converted this cation-selective channel into an anion-selective one [17]. However, little is known about the influence that the ECD plays in ion permeation. In the α7 nAChR, it has been found that the ECD contains a ring of ten aspartates (two per subunit) that is believed to face the lumen of the pore, and which could concentrate cations for permeation [24]. Muscle nAChRs only have five aspartate residues in this region and display a lower calcium permeability than α7 nAChRs [24]. Therefore, we tested the possible involvement of these residues in the calcium permeability of the rat α7 nAChR. We found that one of these residues (the aspartate at position 44) appears to be essential; mutating it to alanine resulted in a decrease in amplitude for both whole cell and single channel responses, and the complete disappearance of detectable calcium changes in 87 % of the cells tested. This indicates that the ECD of α7 nAChRs plays a key role in calcium permeation.

## Materials and methods

### Hippocampal neuronal primary cultures

Primary hippocampal cultures were chosen for their reliability and the ease of expression of α7 nAChR, we have tried other expression systems, but α7 nAChR does not express as readily and there is too much variability. Primary cultures were prepared as previously reported [6]. Briefly, hippocampi from embryonic day 18 rats were mechanically dissociated after treatment for 30 min at 37 °C with 0.05 % Trypsin EDTA (Gibco, Grand Island, NY). Cells were plated in neurobasal medium (Gibco, Grand Island, NY) supplemented with 10 % fetal bovine serum (FBS; Hyclone, Logan UT) and 1 % Glutamax (Gibco, Grand Island, NY) at 3,500/$mm^2$ in poly-d-lysine-coated (Sigma, St. Louis, MO) coverslips and grown in a humidified atmosphere of 5 % $CO_2$ at 37 °C. Half the media was replaced 24 h after plating and every 72 h thereafter with neurobasal media in which FBS was substituted with 2 % B27 (Gibco, Grand Island, NY). Hippocampal neurons were transfected at *day* in vitro 4 (DIV4) with Ric-3 (enhances the functional expression of α7 nicotinic acetylcholine

receptors [23]), GCaMP3 and either wild-type (WT) or mutated α7 nAChR, using calcium phosphate. Cells were analyzed 24–72 hours after transfection. The timeframe of expression and analysis was chosen to minimize the contribution of endogenous channels which have been shown to require longer than 7 DIV to express in culture [2].

### Measurement of ACh-evoked currents

Coverslips containing transfected neurons were transferred to a chamber containing: 165 mM NaCl, 5 mM KCl, 2 mM $CaCl_2$, 10 mM glucose, 5 mM HEPES, 1 μM atropine (Sigma, St. Louis, MO), and 0.3 μM TTX (Tocris, Bristol, UK); pH was adjusted to 7.3 with NaOH. Bath solution was perfused continuously through the chamber (1 mL volume) at 2 mL/min throughout the experiments. Neurons were visualized using a Nikon Eclipse TE300 microscope equipped for fluorescence detection. Borosilicate patch pipettes (3–6 MΩ) were filled with 120 mM CsCl, 2 mM $MgCl_2$, 0.5 mM EGTA, and 10 mM HEPES; pH was adjusted to 7.3 with CsOH. Currents were recorded at −70 mV. Experiments were performed at room temperature (22 °C). Recordings were done using an Axopatch-200A amplifier connected to a Digidata 1322A and software (pCLAMP v. 10.1) from Axon Instruments. Whole cell currents were filtered at 1 kHz and digitized at 10 kHz with an output gain of 1. ACh was applied using a synthetic quartz perfusion tube (0.7 mm, i.d.) operated by a computer-controlled valve (AutoMate Scientific, Berkeley, CA). Two-second applications of 1 mM ACh were analyzed using Clampfit 10.

Outside-out patch-recording currents were filtered at 2 kHz and digitized at 10 kHz with an output gain of 20. Four-second applications of 100 μM ACh were analyzed using Clampfit 10. Estimation of the single channel amplitudes was done by using all-points histograms that were fitted with Gaussian distributions.

Dose–response measurements were done by applying different concentrations of ACh for 2 s followed by a 30-s wash. We have shown previously that recovery from desensitization takes about 10 s [6]. The concentrations used were 50 μM, 100 μM, 300 μM, and 1 mM ACh. To construct the dose–response curve, the responses were first normalized to the response of 1 mM ACh and fitted using a log (agonist) vs normalized response with a variable slope equation on Graph Pad Prism 5.

Reversal potentials were measured using a step protocol in which the cells were allowed to equilibrate to the different voltages (−80 to +40 mV) for 1 min followed by a 4-s pre-application of 10 μM *N*-(5-chloro-2,4-dimethoxyphenyl)-*N*9-(5-methyl-3-isoxazolyl)-urea (PNU-120596) followed by a 2-s application of 1 mM ACh. Peak currents were normalized to the response at −80 mV and fitted using a linear regression with Graph Pad Prism 5.

The relative Ca permeability ($P_{Ca}/P_{Na}$) was calculated using the GHK equation [32] where *R*, *T*, and *F* are standard thermodynamic parameters, $[Na^+]_o$, $[Ca^{2+}{}_2]_o$ and $[Ca^{2+}{}_{20}]_o$ represent $Na^+$ and $Ca^{2+}$ activities respectively, and $\Delta V_{rev} = V_{rev20} - V_{rev2}$ ($V_{rev20}$ and $V_{rev2}$ represent the reversal potentials determined in an external solution with 20 and 2 mM $Ca^{2+}$, respectively):

$$\frac{P_{\mathrm{Ca}}}{P_{\mathrm{Na}}}=\frac{[\mathrm{Na}^{+}]_{o}(1-e^{\Delta V_{\mathrm{rev}}F/RT})}{4[Ca^{2+}{}_{2}]_{o}e^{\frac{\Delta V_{\mathrm{rev}}F}{\mathrm{RT}}}\left(1+e^{\frac{V_{\mathrm{rev}_{2}}F}{\mathrm{RT}}}\right)^{-1}-4\left[\mathrm{Ca}^{2+}{}_{20}\right]_{o}\left(1+e^{\frac{V_{\mathrm{rev}_{20}}F}{\mathrm{RT}}}\right)^{-1}}$$

[32]

All data are plotted as mean ± SEM and was analyzed using Prism 5 (Graph Pad, La Jolla, CA).

### Imaging of intracellular [$Ca^{2+}$]

Changes in calcium concentration due to the application of ACh were assessed using fluorescence imaging and GCaMP3. GCaMP3 has been shown to have very good signal to noise ratio, protein stability, sensitivity, and fast kinetics [39]. Furthermore, the use of GCaMP3 as our calcium indicator facilitated easy identification of the cells that were transfected, by looking at the basal fluorescence. Combining fluorescence microscopy and electrophysiology has been used previously to study the calcium permeability of nAChRs using different calcium indicators [13, 15]. Images were captured with a Luca R camera (Andor) using a Nikon Eclipse TE300 microscope equipped with fluorescence detection. The Andor iQ imaging program was used to capture, store and later analyze the changes in fluorescence intensity; 2×2 image binning was used to increase the signal to noise ratio and time resolution (10 frames/s). The level of intracellular free calcium was expressed as the ratio of peak fluorescence over the basal fluorescence ($\Delta F/F$) [13, 15].

## Results

### Effects of mutations in the ECD on α7 nAChR channel function

The crystal structure from a chimera composed of the ECD of the human α7 nAChR and the acetylcholine-binding protein (AChBP) uncovered the existence of inter-subunit interactions between a lysine residue (Lys 44) and an aspartate residue (Asp 40) from contiguous subunits. These residues are believed to face the lumen of the pore, and the presence of another aspartate (Asp 42) residue in this region is believed to contribute to the formation of a strong negative potential that could play a role attracting cations and increasing their permeability through the channel (see [24] for location and structural organization of this region). To study the possible involvement of these residues in the calcium permeability of the α7 nAChR, we created mutants in which these charged residues were replaced with alanine (A) at the homologous sites of the rat α7 nAChR; Asp 42 (D42A), Asp 44 (D44A), and Lys 46 (K46A; homologous to D40, D42, and K44 in human α7 nAChR).

Cultured hippocampal neurons coexpressing GCaMP3, Ric3 and either WT or mutated rat α7 nAChR, were exposed to a 2-s rapid application of ACh (1 mM) at a holding potential of −70 mV; this resulted in the activation of a fast inward current that desensitized completely in the continued presence of agonist. Acetylcholine-evoked responses in WT displayed a mean amplitude of −1,321±113 pA, with a desensitization half-time of 42±3 ms (Fig. 1). As reported previously, the onset of desensitization was biphasic [22]; the fast component ( $\tau_{\mathrm{fast}}$

=29±2 ms) comprised 77±2 %, while the slow component ( $\tau_{slow}$=384±32 ms) comprised 11±1 % of the total desensitization (Fig. 1b).

All of the α7 nAChR mutants tested in this study were able to form functional channels, however the characteristics of the responses varied. The current amplitude of the D44A mutant was significantly decreased (−467±34 vs −1,321±113 pA for WT), whereas there was no significant difference in amplitude for either the D42A or K46A mutants (Fig. 1a). Interestingly, the desensitization half-time was not affected in the D44A mutant (43±3 vs 42±3 ms for WT) but was significantly increased for both the D42A and K46A mutants (62±10 and 85±4 ms, respectively) (Fig. 1b). The fast desensitization time constant for the K46A was 58±4 ms, which was significantly slower than WT ( $\tau_{fast}$=29±2 ms). In addition there was a significant increase in the slow component of desensitization for the K46A mutant (24 ± 2 vs 11 ± 1 % for WT), accompanied by a significant decrease in the fast component (68±2 vs 77±2 % for WT). These data indicate that the K46A mutant desensitizes at a significantly slower rate than WT receptors. For the D44A mutant, while neither half-time nor time constants of desensitization were different from the WT receptors, there was a significant increase in the fast component of desensitization (85±2 vs 77±2 % for WT) and a significant decrease in the slow component of desensitization (5±1 vs 11±1 % for WT) (Fig. 1b).

As the residues mutated in this study were located in the ECD of the α7 nAChR, which contains the ligand-binding site, we tested whether the potency of the α7 nAChR for ACh was affected. Dose–response curves were constructed and indicated that all mutants displayed a small decrease in agonist affinity when compared with WT receptors ($EC_{50}$ =109 μM, log $EC_{50}$=2.04±0.03, and hill slope=1.67±0.20); D42A ($EC_{50}$= 142 μM, log $EC_{50}$ =2.15±0.02, and hill slope=1.78±0.17; $p$ = 0.034); D44A ($EC_{50}$=153 μM, log $EC_{50}$ =2.19±0.03, and hill slope=1.69±0.18; $p$ =0.007); K46A ($EC_{50}$=145 μM, log $EC_{50}$ =2.16±0.03, and hill slope=1.80±0.19; $p$ =0.025) (Fig. 1c).

## Mutations to the ECD of the α7 nAChR reduce calcium permeability

The ion selectivity filter of the nAChR has been studied extensively using site directed mutagenesis to identify the contribution of different residues to ion conductance and selectivity. Thus far the results suggest that rings of negatively charged amino acids within the pore lining M2 domain are the main determinant of nAChR's ionic permeability [7, 14].

The α7 nAChR is the most prevalent hippocampal nAChR subtype with the highest calcium permeability among native nAChRs [5]. Residues in the M2 transmembrane region of this receptor have been shown to be critical for calcium permeability. For example, the E237A mutation in the chick α7 nAChR abolishes calcium permeability without significantly affecting other channel properties [4]. However, little is known about the possible involvement of the ECD of the α7 nAChR to ionic permeability. Therefore, we decided to look at the effect of the mutations described above on calcium permeability by using simultaneous recordings of transmembrane currents and fluorescence calcium transients [13, 15].

Calcium entry into the cells was monitored by measuring the fluorescence changes using a digital camera and the genetically encoded calcium indicator, GCaMP3. To compare the relative calcium permeability during the activation of WT and mutated α7 nAChRs, we plotted the peak increase in fluorescence change ($\Delta F/F$; which is indicative of increases in cytoplasmic calcium levels) versus the integrated membrane current (charge ($Q$); Fig. 2a). The slope of this line for either the K46A or D42A mutant was not significantly different from WT (Fig. 2b). Interestingly, the D44A mutant shows a complete lack of calcium permeability (i.e. detectable calcium responses) in 87 % of the cells tested (27 of 31 cells show no change in fluorescence, while the other four show a detectable change). As the amplitude of current responses for the D44A mutant was significantly smaller than for WT receptors, we compared the ratio of the calcium response to charge ($F/Q$ ratio) and found that differences still persisted for the D44A mutant, but neither the K46A nor D42A mutants (data not shown). This suggests that the aspartate at position 44 is critical for calcium permeability of the α7 nAChRs.

Although there is a clear reduction in the GCaMP3 fluorescence caused by the D44A mutant, to confirm this potential reduction in calcium permeability, we determined the reversal potential ($V_{rev}$) for WT and D44A mutant α7 nAChRs at different calcium concentrations (2 and 20 mM $Ca^{2+}$), and used the change in $V_{rev}$ to calculate the permeability ratios ($P_{Ca}/P_{Na}$). For these experiments, it was necessary to use the α7-positive allosteric modulator PNU-120596 to potentiate the responses for the D44A mutant; these responses were significantly smaller than WT, which made it extremely difficult to accurately measure response amplitudes near the $V_{rev.}$ PNU-120596 has been previously shown to reduce the inward rectification without affecting the divalent cation permeability [29]. Consistent with a reduction in the calcium permeability for the D44A mutant, the shift in $V_{rev}$ ($\Delta V_{rev}$) determined by fitting the I–V curves was 16.1 mV for WT (Fig. 2c) and 6.6 mV for the D44A mutant α7 nAChRs (Fig. 2d), which corresponded to a 64 % reduction in the relative calcium permeability ($P_{Ca}/P_{Na}$) for the D44A mutant versus WT α7 nAChR.

## Mutations to the ECD of the α7 nAChR affect single-channel behavior

Calcium ions have been shown to have a high affinity and influence the conductance of muscle nAChRs [10]; however, it is unclear if there is any correlation between the calcium permeability and conductance of neuronal nAChRs. Therefore, we investigated what effects these ECD mutations have on the single channel behavior of α7 nAChRs in outside-out membrane patches that were exposed to a 4 s rapid application of ACh (100 μM) at a holding potential of −70 mV.

For neurons expressing WT α7 nAChRs, agonist application evoked single channel activity that appears as isolated brief openings with a mean open time of 0.32 ms and a mean amplitude of −4.0 pA (Fig. 3a, c, d). Mutations to the Lys 46 and the Asp 42 residues showed no significant differences in either mean open time (0.32±0.01, 0.38±0.01, and 0.34±0.01 ms for WT, D42A, and K46A, respectively), or mean amplitude (−4.0±0.05, −3.7±0.05, and 4.5±0.05 pA for WT, D42A, and K46A, respectively)(Fig. 3b). However the D44A mutant displayed significantly longer mean open times (0.81±0.03 ms; Fig. 3c) and significantly reduced mean amplitudes (−2.5±0.02 vs −4.0±0.05 pA for WT) (Fig. 3c, d),

indicating that this residue is crucial for both gating and the calcium permeability of the α7 nAChR.

## Discussion

Much recent evidence clearly indicates that the α7 nAChRs are involved in regulating synaptic excitability, plasticity, and learning and memory processes in the hippocampus [18, 19, 40].This role may in part be due to the high calcium permeability of this receptor and increases in cytoplasmic calcium levels, which can impact many cellular events including neurotransmitter release, second messenger cascades, cell survival and apoptosis. While much evidence indicates that key residues in the M2 domain and the intracellular loop of the channel are involved in cationic selectivity and permeation [7, 17], including the glutamate at residue 237 of the α7 nAChR that when mutated to alanine abolishes calcium permeability of this receptor [4], little is known about the influence that the ECD plays in ion permeation. Recently, the α7 nAChRs have emerged as potential targets in the treatment of many neurological disorders, such as Parkinson's and Alzheimer's diseases, and schizophrenia, and even for chemotherapy-induced cognitive impairments [15, 21, 31, 41]. Furthermore, it has been shown that α7 nAChRs are expressed in macrophages where they play a key role in the cholinergic anti-inflammatory pathway [45], and they have proven to be an effective target in the treatment of sepsis, myocardial ischemia, and rheumatoid arthritis [30]. There is a critical need for improving our understanding of the structure-function relationship of α7 nAChRs to improve our chances of successfully targeting them for therapeutic purposes, as well as understanding their role in regulating synaptic excitability and plasticity.

In a recent study, looking at the crystal structure of the ECD of the α7 nAChR by creating a chimera with AChBP, Li et al. [24] found intersubunit electrostatic interactions involving the lysine at position 44 and the aspartate at position 40 of the human α7 nAChR. Furthermore, these residues are specific for certain neuronal nAChRs. In combination with another aspartate at position 42, these residues create a negative potential that faces the lumen of the pore, which Li et al. [24] suggested could impact the ionic permeability of the α7 nAChR. We investigated the involvement of these residues in the calcium permeability of the α7 nAChR using mutagenesis to replace these charged residues with an uncharged alanine residue. We found that mutating the aspartate residue at position 44 of the rat α7 nAChR (which corresponds to residue 42 in the human receptor) dramatically reduced the calcium permeability of the α7 nAChR, resulting in a significant reduction in the shift in $V_{rev}$ ($\Delta V_{rev}$) on a high vs low calcium solution (16.1 vs 6.6 mV in WT and D44A mutant respectively), and the complete lack of apparent calcium permeability (measured as a lack of change in GCaMP3 fluorescence levels) in 87 % of the cells tested. Mutating either the Asp 42 or Lys 46 residues had no significant effect on calcium permeability, although the K46A mutant affected the desensitization kinetics. As Asp 42 was found to form an electrostatic interaction with Lys 46 from the adjacent subunit, this interaction either hinders the ability of Asp 42 to interact with calcium ions, or instead this interaction may be necessary for the normal function of the α7 nAChR as the ligand-binding domain of nAChRs establishes a major communication link with the pore domain [24]. Interestingly, two aspartate residues in the ECD of the 5-$HT_3$ A receptor were shown through mutagenesis to influence calcium

permeability, supporting the idea that the ECD plays an important role in the ionic permeability of ligand gated ion channels [25].

The influx of calcium ions through the α7 nAChRs has implications for regulating various signal transduction cascades and synaptic plasticity [9, 14]. Recently, we found that properly-timed endogenous ACh release can induce LTP via activation of α7 nAChRs (in either acute or cultured hippocampal slices [18, 19], and this was dependent on the prolongation of the NMDAR-mediated calcium transients in CA1 pyramidal neuron spines; this may in part have been due to calcium influx through the α7 nAChRs. Increases in cytoplasmic calcium levels through the α7 nAChRs have been shown to activate CaMK and MAPK pathways, leading to the activation of CREB and gene expression [20], and downregulates $GABA_A$ receptor-induced currents via calcium-dependent cascades [43, 46]. Furthermore, we and others have shown that the activation of the α7 nAChRs on astrocytes in the hippocampus increases cytoplasmic calcium levels [33, 36, 42]. This might be significant since α7 nAChRs are thought to be participating in various mechanisms of neuroprotection [12, 28, 35], perhaps via the calcium-dependent phosphatase calcineurin [8, 38]. The prolonged or excessive activation of α7 receptors can also lead to calcium overload and excitotoxicity [16, 26, 27]. Therefore, the spatiotemporal dynamics of cytoplasmic calcium levels, and how they are regulated by nAChRs, will be critical in understanding the effects that calcium influx is having on synaptic excitability and plasticity, as well as neuroprotection and excitotoxicity.

In conclusion, we have shown that the aspartate at residue 44 of the rat α7 nAChR appears to be critical for calcium permeability, which indicates that the ECD of the α7 nAChR plays a key role in calcium permeation. Furthermore, this provides an experimental tool to probe what impact calcium influx through the α7 nAChR has on synaptic excitation and plasticity, as well as in neuroprotection.

## Acknowledgments

This work was supported by the Intramural Research Program of the National Institute of Environmental Health Sciences (NIEHS). The authors also thank Dr. Ezequiel Marron and Dr. Christian Erxleben for their helpful insights and suggestions in the manuscript preparation process and Pattie Lamb for preparing all of the constructs used in this study.

## References

1. Absalom NL, Schofield PR, Lewis TM. Pore structure of the Cys-loop ligand-gated ion channels. Neurochem Res. 2009; 34:1805–1815. [PubMed: 19381804]
2. Arnaiz-Cot JJ, Gonzalez JC, Sobrado M, Baldelli P, Carbone E, Gandia L, Garcia AG, Hernandez-Guijo JM. Allosteric modulation of alpha 7 nicotinic receptors selectively depolarizes hippocampal interneurons, enhancing spontaneous GABAergic transmission. Eur J Neurosci. 2008; 27:1097–1110. [PubMed: 18312591]
3. Berger F, Gage FH, Vijayaraghavan S. Nicotinic receptor-induced apoptotic cell death of hippocampal progenitor cells. J Neurosci. 1998; 18:6871–6881. [PubMed: 9712657]
4. Bertrand D, Galzi JL, Devillers-Thiery A, Bertrand S, Changeux JP. Mutations at two distinct sites within the channel domain M2 alter calcium permeability of neuronal alpha 7 nicotinic receptor. Proc Natl Acad Sci U S A. 1993; 90:6971–6975. [PubMed: 7688468]
5. Castro NG, Albuquerque EX. Alpha-Bungarotoxin-sensitive hippocampal nicotinic receptor channel has a high calcium permeability. Biophys J. 1995; 68:516–524. [PubMed: 7696505]

6. Colon-Saez JO, Yakel JL. The alpha7 nicotinic acetylcholine receptor function in hippocampal neurons is regulated by the lipid composition of the plasma membrane. J Physiol. 2011; 589:3163–3174. [PubMed: 21540349]
7. Corringer PJ, Le Novere N, Changeux JP. Nicotinic receptors at the amino acid level. Annu Rev Pharmacol Toxicol. 2000; 40:431–458. [PubMed: 10836143]
8. Dajas-Bailador FA, Lima PA, Wonnacott S. The alpha7 nicotinic acetylcholine receptor subtype mediates nicotine protection against NMDA excitotoxicity in primary hippocampal cultures through a Ca(2+) dependent mechanism. Neuropharmacology. 2000; 39:2799–2807. [PubMed: 11044750]
9. Dajas-Bailador F, Wonnacott S. Nicotinic acetylcholine receptors and the regulation of neuronal signalling. Trends Pharmacol Sci. 2004; 25:317–324. [PubMed: 15165747]
10. Decker ER, Dani JA. Calcium permeability of the nicotinic acetylcholine receptor: the single-channel calcium influx is significant. J Neurosci. 1990; 10:3413–3420. [PubMed: 2170596]
11. Delbono O, Gopalakrishnan M, Renganathan M, Monteggia LM, Messi ML, Sullivan JP. Activation of the recombinant human α7 nicotinic acetylcholine receptor significantly raises intracellular free calcium. J Pharmacol Exp Ther. 1997; 280:428–438. [PubMed: 8996225]
12. Dineley KT. Beta-amyloid peptide–nicotinic acetylcholine receptor interaction: the two faces of health and disease. Front Biosci. 2007; 12:5030–5038. [PubMed: 17569627]
13. Fayuk D, Yakel JL. $Ca^{2+}$ permeability of nicotinic acetylcholine receptors in rat hippocampal CA1 interneurones. J Physiol. 2005; 566:759–768. [PubMed: 15932886]
14. Fucile S. $Ca^{2+}$ permeability of nicotinic acetylcholine receptors. Cell Calcium. 2004; 35:1–8. [PubMed: 14670366]
15. Fucile S, Palma E, Mileo AM, Miledi R, Eusebi F. Human neuronal threonine-for-leucine-248 alpha 7 mutant nicotinic acetylcholine receptors are highly $Ca^{2+}$ permeable. Proc Natl Acad Sci U S A. 2000; 97:3643–3648. [PubMed: 10716716]
16. Fucile S, Sucapane A, Grassi F, Eusebi F, Engel AG. The human adult subtype ACh receptor channel has high $Ca^{2+}$ permeability and predisposes to endplate $Ca^{2+}$ overloading. J Physiol. 2006; 573:35–43. [PubMed: 16527851]
17. Galzi JL, Devillers-Thiery A, Hussy N, Bertrand S, Changeux JP, Bertrand D. Mutations in the channel domain of a neuronal nicotinic receptor convert ion selectivity from cationic to anionic. Nature. 1992; 359:500–505. [PubMed: 1383829]
18. Gu Z, Lamb PW, Yakel JL. Cholinergic coordination of presynaptic and postsynaptic activity induces timing-dependent hippocampal synaptic plasticity. J Neurosci. 2012; 32:12337–12348. [PubMed: 22956824]
19. Gu Z, Yakel JL. Timing-dependent septal cholinergic induction of dynamic hippocampal synaptic plasticity. Neuron. 2011; 71:155–165. [PubMed: 21745645]
20. Hu M, Liu QS, Chang KT, Berg DK. Nicotinic regulation of CREB activation in hippocampal neurons by glutamatergic and nonglutamatergic pathways. Mol Cell Neurosci. 2002; 21:616–625. [PubMed: 12504594]
21. Kawamata J, Suzuki S, Shimohama S. Alpha7 nicotinic acetylcholine receptor mediated neuroprotection in Parkinson's disease. Curr Drug Targets. 2012; 13:623–630. [PubMed: 22300030]
22. Khiroug SS, Harkness PC, Lamb PW, Sudweeks SN, Khiroug L, Millar NS, Yakel JL. Rat nicotinic ACh receptor alpha7 and beta2 subunits co-assemble to form functional heteromeric nicotinic receptor channels. J Physiol. 2002; 540:425–434. [PubMed: 11956333]
23. Lansdell SJ, Gee VJ, Harkness PC, Doward AI, Baker ER, Gibb AJ, Millar NS. RIC-3 enhances functional expression of multiple nicotinic acetylcholine receptor subtypes in mammalian cells. Mol Pharmacol. 2005; 68:1431–1438. [PubMed: 16120769]
24. Li S-X, Huang S, Bren N, Noridomi K, Dellisanti CD, Sine SM, Chen L. Ligand-binding domain of an [alpha]7-nicotinic receptor chimera and its complex with agonist. Nat Neurosci. 2011; 14:1253–1259. [PubMed: 21909087]
25. Livesey MR, Cooper MA, Lambert JJ, Peters JA. Rings of charge within the extracellular vestibule influence ion permeation of the 5-HT3A receptor. J Biol Chem. 2011; 286:16008–16017. [PubMed: 21454663]

26. Lukas RJ, Lucero L, Buisson B, Galzi JL, Puchacz E, Fryer JD, Changeux JP, Bertrand D. Neurotoxicity of channel mutations in heterologously expressed alpha7-nicotinic acetylcholine receptors. Eur J Neurosci. 2001; 13:1849–1860. [PubMed: 11403678]
27. Ng HJ, Whittemore ER, Tran MB, Hogenkamp DJ, Broide RS, Johnstone TB, Zheng L, Stevens KE, Gee KW. Nootropic alpha7 nicotinic receptor allosteric modulator derived from GABAA receptor modulators. Proc Natl Acad Sci U S A. 2007; 104:8059–8064. [PubMed: 17470817]
28. Parri HR, Hernandez CM, Dineley KT. Research update: alpha7 nicotinic acetylcholine receptor mechanisms in Alzheimer's disease. Biochem Pharmacol. 2011; 82:931–942. [PubMed: 21763291]
29. Peng C, Kimbrell MR, Tian C, Pack TF, Crooks PA, Fifer EK, Papke RL. Multiple modes of α7 nAChR noncompetitive antagonism of control agonist-evoked and allosterically enhanced currents. Mol Pharmacol. 2013; 84:459–475. [PubMed: 23839567]
30. Pohanka M. Alpha7 nicotinic acetylcholine receptor is a target in pharmacology and toxicology. Int J Mol Sci. 2012; 13:2219–2238. [PubMed: 22408449]
31. Raffa RB. Cancer 'survivor-care': I. the alpha7 nAChR as potential target for chemotherapy-related cognitive impairment. J Clin Pharm Ther. 2011; 36:437–445. [PubMed: 21729110]
32. Ragozzino D, Barabino B, Fucile S, Eusebi F. $Ca^{2+}$ permeability of mouse and chick nicotinic acetylcholine receptors expressed in transiently transfected human cells. J Physiol. 1998; 507:749–757. [PubMed: 9508836]
33. Sharma G, Vijayaraghavan S. Nicotinic cholinergic signaling in hippocampal astrocytes involves calcium-induced calcium release from intracellular stores. Proc Natl Acad Sci U S A. 2001; 98:4148–4153. [PubMed: 11259680]
34. Sharma G, Vijayaraghavan S. Modulation of presynaptic store calcium induces release of glutamate and postsynaptic firing. Neuron. 2003; 38:929–939. [PubMed: 12818178]
35. Shen JX, Tu B, Yakel JL. Inhibition of alpha 7-containing nicotinic ACh receptors by muscarinic M1 ACh receptors in rat hippocampal CA1 interneurones in slices. J Physiol. 2009; 587:1033–1042. [PubMed: 19124535]
36. Shen JX, Yakel JL. Functional alpha7 nicotinic ACh receptors on astrocytes in rat hippocampal CA1 slices. J Mol Neurosci. 2012; 48:14–21. [PubMed: 22351110]
37. Shimohama S, Kihara T. Nicotinic receptor-mediated protection against beta-amyloid neurotoxicity. Biol Psychiatry. 2001; 49:233–239. [PubMed: 11230874]
38. Stevens TR, Krueger SR, Fitzsimonds RM, Picciotto MR. Neuroprotection by nicotine in mouse primary cortical cultures involves activation of calcineurin and L -type calcium channel inactivation. J Neurosci. 2003; 23:10093–10099. [PubMed: 14602824]
39. Tian L, Hires SA, Mao T, Huber D, Chiappe ME, Chalasani SH, Petreanu L, Akerboom J, McKinney SA, Schreiter ER, Bargmann CI, Jayaraman V, Svoboda K, Looger LL. Imaging neural activity in worms, flies and mice with improved GCaMP calcium indicators. Nat Meth. 2009; 6:875–881.
40. Timofeeva OA, Levin ED. Glutamate and nicotinic receptor interactions in working memory: importance for the cognitive impairment of schizophrenia. Neuroscience. 2012; 195:21–36. [PubMed: 21884762]
41. Toyohara J, Hashimoto K. alpha7 Nicotinic Receptor Agonists: Potential Therapeutic Drugs for Treatment of Cognitive Impairments in Schizophrenia and Alzheimer's Disease. Open Med Chem J. 2010; 4:37–56. [PubMed: 21249164]
42. Velez-Fort M, Audinat E, Angulo MC. Functional alpha 7-containing nicotinic receptors of NG2-expressing cells in the hippocampus. Glia. 2009; 57:1104–1114. [PubMed: 19170184]
43. Wanaverbecq N, Semyanov A, Pavlov I, Walker MC, Kullmann DM. Cholinergic axons modulate GABAergic signaling among hippocampal interneurons via postsynaptic alpha7 nicotinic receptors. J Neurosci. 2007; 27:5683–5693. [PubMed: 17522313]
44. Wang HL, Cheng X, Taylor P, McCammon JA, Sine SM. Control of cation permeation through the nicotinic receptor channel. PLoS Comput Biol. 2008; 4:e41. [PubMed: 18282090]
45. Wang H, Yu M, Ochani M, Amella CA, Tanovic M, Susarla S, Li JH, Wang H, Yang H, Ulloa L, Al-Abed Y, Czura CJ, Tracey KJ. Nicotinic acetylcholine receptor [alpha]7 subunit is an essential regulator of inflammation. Nature. 2003; 421:384–388. [PubMed: 12508119]

46. Zhang J, Berg DK. Reversible inhibition of GABAA receptors by alpha7-containing nicotinic receptors on the vertebrate postsynaptic neurons. J Physiol. 2007; 579:753–763. [PubMed: 17204496]

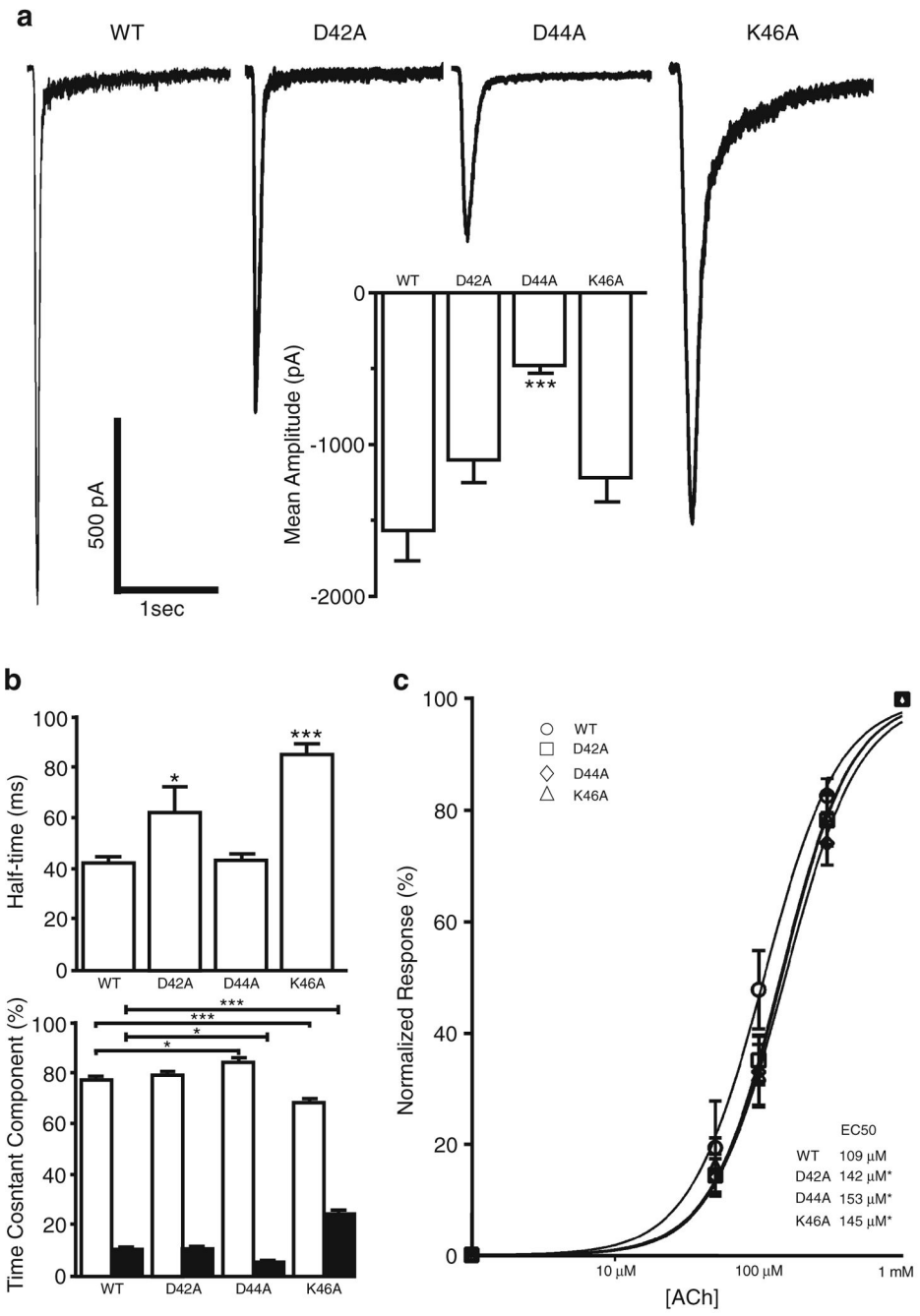


**Fig. 1.**

Effects of mutations to the ECD on α7 nAChR channel function. Hippocampal neurons coexpressing Ric3, GCaMP3, and either WT or mutated α7 nAChR were subjected to a 2-s application of 1 mM ACh. **a** Representative responses to ACh application in WT (*n* =62), D42A (*n* =42), D44A (*n* =34), and K46A (*n* =36) mutants. Mean amplitude was significantly reduced for the D44A mutant (*insert*). **b** D42A and K46A mutants displayed slower desensitization half-times. Desensitization time constants ($\tau$) were calculated using Clampfit and fitted with a two exponential equation. K46A mutation results in an increase in

the fast desensitization time constant ( $\tau_{fast}$=58±4 vs 29±2 ms in WT). Interestingly, K46A and D44A had opposite effects on the ratio of fast and slow desensitization. **c** Neurons were subjected to consecutive 2 s applications of 50 μM, 100 μM, 300 μM, and 1 mM ACh. Responses were normalized to the response to 1 mM ACh. Dose–response curves were constructed from WT (*n* =9), D42A (*n* =9), D44A (*n* = 11), and K46A (*n* =11) mutants and compared using Graph Pad Prism 5. All Plots show mean±SEM and were subjected to a one-way ANOVA analysis; ****p* < 0.0001; **p* <0.05. **c** Log $EC_{50}$ was compared using a Log (agonist) versus normalized response with variable slope fit in Graph Pad Prism 5; **p* <0.05

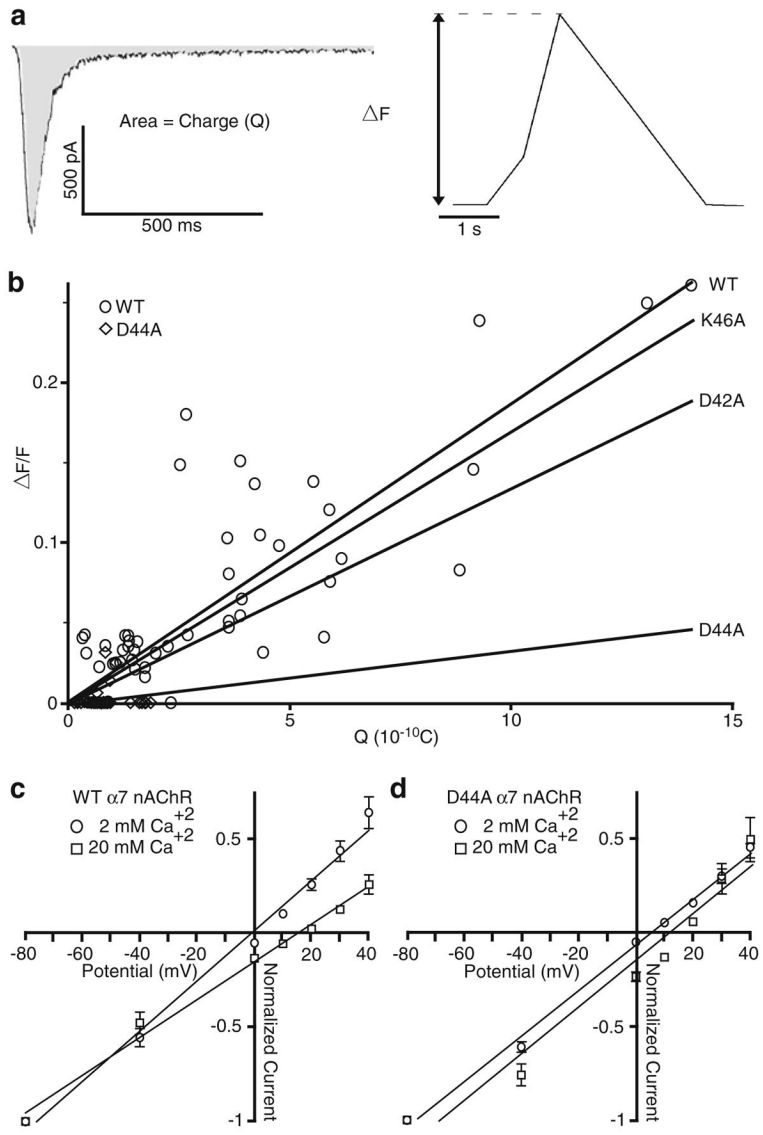


**Fig. 2.**

Mutations to the ECD of α7 nAChR reduce calcium permeability. Hippocampal neurons coexpressing Ric3, GCaMP3, and either WT or mutated α7 nAChR were subjected to a 2-s application of 1 mM ACh and assessed for both their electrophysiological and fluorescence responses. Changes in intracellular calcium concentration were assessed using fluorescence imaging and GCaMP3. **a** The level of intracellular free calcium (expressed as the ratio of peak fluorescence over the basal fluorescence (Δ*F*/*F*)) is proportional to the integrated membrane current (charge, *Q*), which is estimated as the area under the current trace. **b** The plot of the intracellular free calcium and the integrated current yields a near linear relationship (shown is WT and D44A actual data; and the linear regression for WT (*n* =56; $R_{val}$=0.4759), D42A (*n* =34; $R_{val}$= 0.05222), D44A (*n* =31; $R_{val}$=0.006528), and K46A (*n* =33; $R_{val}$= 0.2147)). **c**, **d** The reversal potential ($V_{rev}$) was measured using external solutions containing 2 and 20 mM $Ca^{2+}$ for WT and D44A mutant, using a 4-s pre-application of 10 μM PNU-120596 and a 2-s application of 1 mM ACh. **c** The current–voltage relationship of

WT α7 nAChR showed an $V_{rev}$ of −1.1 ($n$ =6; $R_{val}$=0.9901) and 15 mV ($n$ =8; $R_{val}$= 0.9915) at 2 and 20 mM $Ca^{2+}$, respectively. **d** The current–voltage relationship of the D44A mutant α7 nAChR showed an $V_{rev}$ of 5.6 ($n$ = 8; $R_{val}$=0.9959) and 12.2 mV ($n$ = 7; $R_{val}$=0.9547) at 2 and 20 mM $Ca^{2+}$, respectively. To calculate the $V_{rev}$, peak currents were normalized to the response at −80 mV and fitted using a linear regression with Graph Pad Prism 5. All data are plotted as mean±SEM

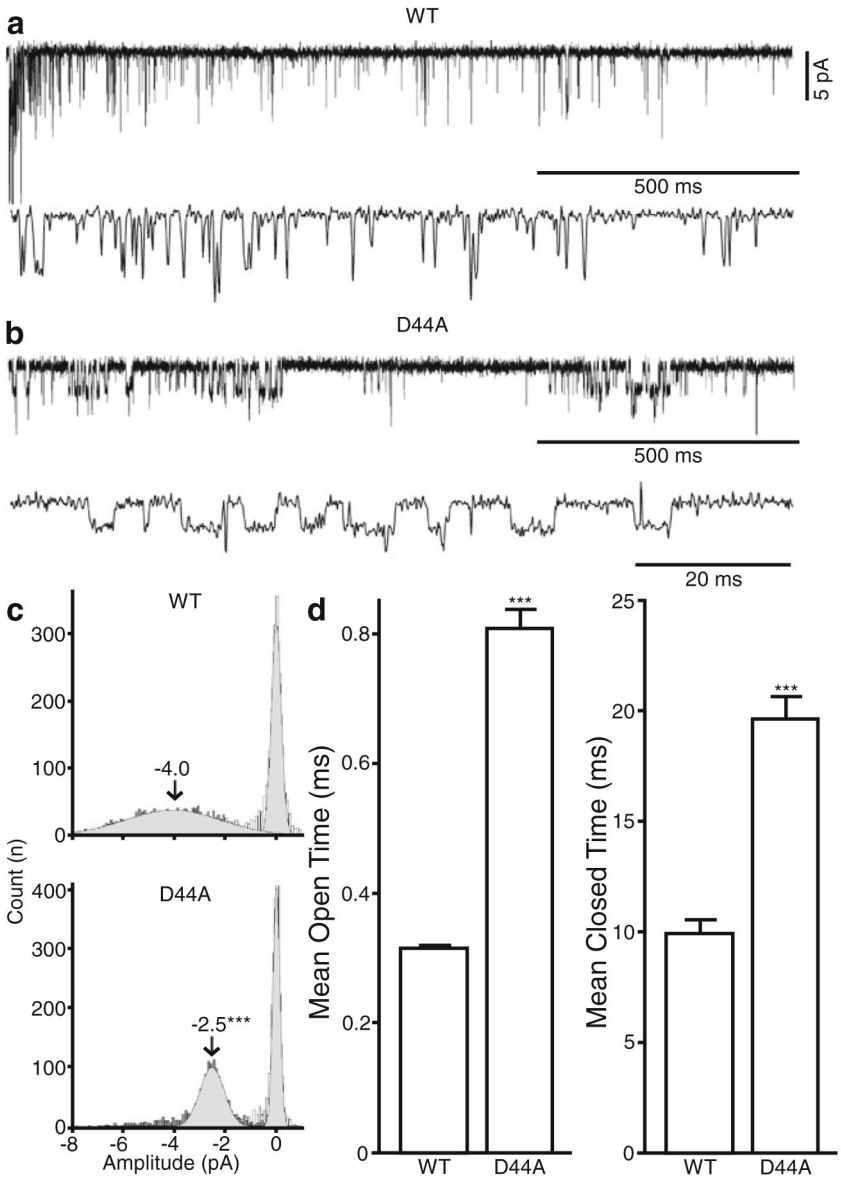


**Fig. 3.**

Mutations to the ECD of α7 nAChR affect single-channel behavior. Hippocampal neurons coexpressing Ric3, GCaMP3, and either WT or mutated α7 nAChR were subjected to a 4-s application of 100 μM ACh. **a**, **b** Single-channel traces from WT and D44A using the outside-out configuration. **c** All points histogram of amplitudes of the single channel current from WT (five patches), D42A (six patches), D44A (five patches), and K46A (ten patches). The mean amplitudes were calculated using a single exponential Gaussian fit and compared using Graph Pad Prism 5. **d** Mean open times were compared in WT and D44A mutant patches. Plots show mean±SEM and were subjected to a *t* test analysis; ***$p$ <0.0001